197

United States
Department of
Agriculture

Forest Service

Technology &
Development
Program

3400–Forest Pest
Management
September 1989
MTDC 89-28

AGDISP and FSCBG Aerial Spray Model–Source Decay Coefficients

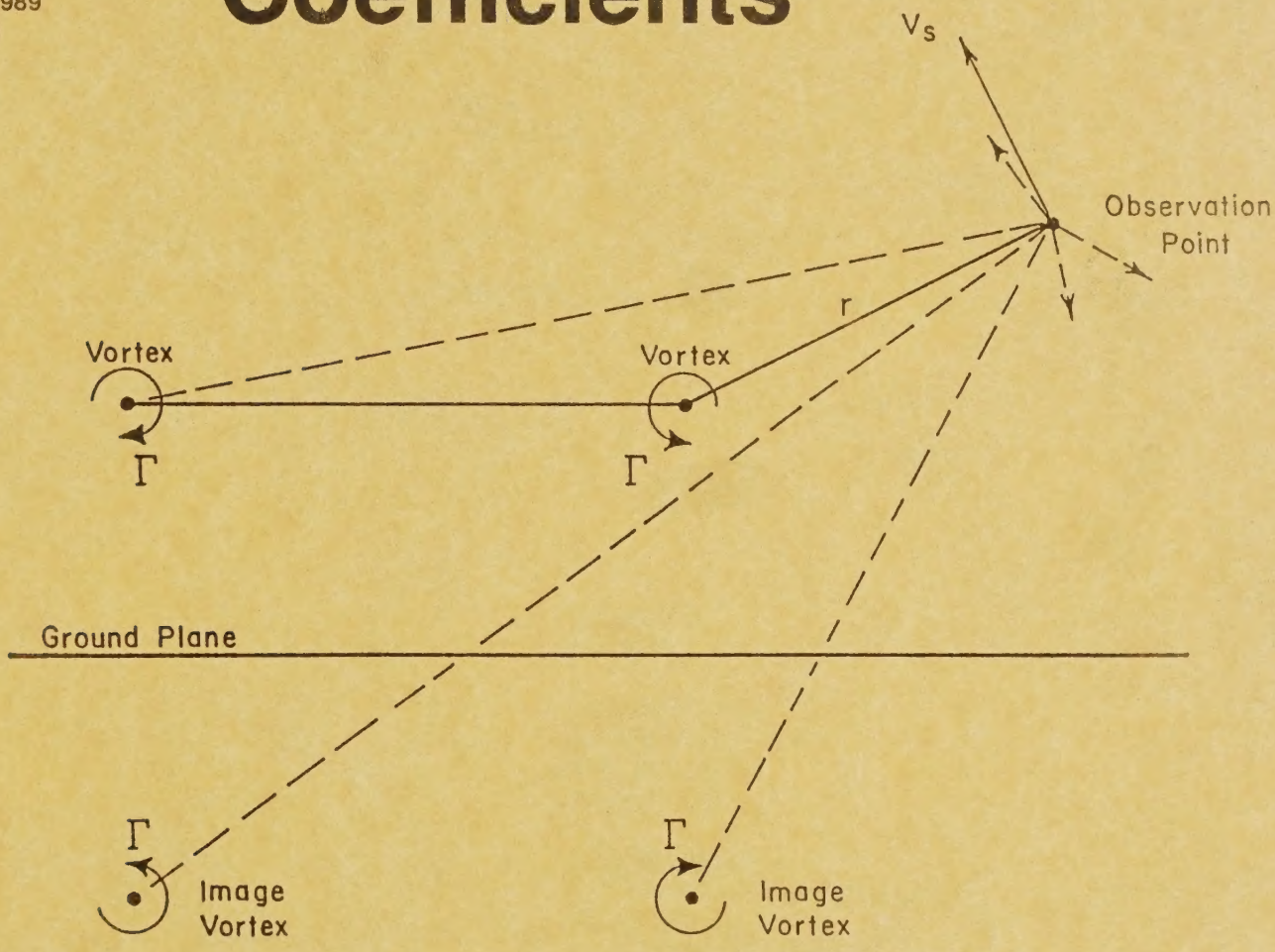

AGDISP and FSCBG Aerial Spray Model–Source Decay Coefficients

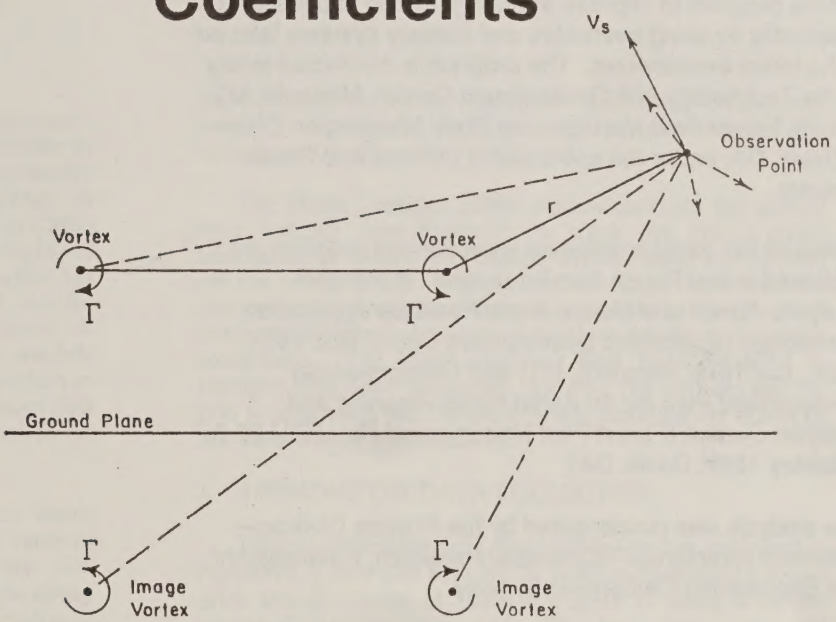

Prepared by
Milton E. Teske

Alan J. Bilanin
Continuum Dynamics
P.O. Box 3073
Princeton, NJ

John W. Barry
U.S. Department of Agriculture
Forest Service
Forest Pest Management
Davis, CA

Robert B. Ekblad
U.S. Department of Agriculture
Forest Service
Technology and Development Center
Missoula, MT

Pesticide Precautionary Statement

This publication reports research involving pesticides. It does not contain recommendations for their use, nor does it imply that the uses discussed here have been registered. All uses of pesticides must be registered by appropriate State and/or Federal agencies before they can be recommended.

Caution: Pesticides can be injurious to humans, domestic animals, desirable plants, and fish or other wildlife—if they are not handled or applied properly. Use all pesticides selectively and carefully. Follow recommended practices for the disposal of surplus pesticides and pesticide containers.

Foreword

This report is published as a part of the USDA Forest Service program to improve aerial application of pesticides, specifically by using pesticides and delivery systems tailored to the forest environment. The program is conducted jointly by the Technology and Development Center, Missoula, MT, and the Forest Pest Management Staff, Washington Office at Davis, CA, under the sponsorship of State and Private Forestry.

Details of the aerial application improvement program are explained in two Forest Service reports: *A Problem Analysis: Forest and Range Aerial Pesticide Application Technology* (Equipment Development Center Rpt. 7934 2804, July 1979, Missoula, MT) and *Recommended Development Plan for An Aerial Spray Planning and Analysis System* (Forest Pest Management Rpt. FPM 82-2, February 1982, Davis, CA).

The analysis was cosponsored by the Physics Division—Research Directorate—(Chemical Research, Development and Engineering Center)—U.S. Army.

The study was conducted as part of Program WIND (winds in nonuniform domains). Authority for the cooperative program is the Supplemental Agreement, dated February 1985, to the master Memorandum of Understanding Between U.S. Department of Defense and U.S. Department of Agriculture Relative to Cooperation with Respect to Food, Agriculture, and Other Research of Mutual Interest.

1. SUMMARY

In Phases I and III of Project WIND anemometer tower grids recorded the ambient vertical velocity time histories as various fixed-wing aircraft and helicopters repeatedly traversed normal to the grid. Tower grids were present in the open fields and forest at Foresthill, the orchard at Chico and drainage downslope at Red Bluff. These digitized velocity traces produced aircraft wake signature data that has been used to infer vortex strength and lateral and vertical motion of the aircraft vortex pairs generating the traces. A numerical algorithm consistent with the wake models implemented into the AGDISP and FSCBG predictive computer codes has been used to examine this extensive data base of 328 flybys, to infer the wake decay properties in the atmosphere with and without canopy effects.

The quantity defined by decay coefficient times turbulence level is well correlated to have a mean value of 0.56 m/sec and a standard deviation of 0.32 m/sec. For the turbulence levels determined at the test sites, the decay coefficient is seen to vary between near-zero to a value of 2.0 . This result correlates well with a theoretical atmospheric decay coefficient of 0.41 .

2. INTRODUCTION

Project WIND ("Winds in Nonuniform Domains") was performed in phases jointly by the United States Department of Agriculture Forest Service and the United States Army at several sites in northern California. Phase I was conducted from May through July, 1985 at a cleared and forested site (Foresthill Seed Orchard) and an almond orchard (Hennigan Almond Orchard north of Chico); and Phase III, from late April to early May, 1986 at a cleared sloping site in the Sierra Nevada foothills near Red Bluff. In both of these experimental studies, anemometer tower grids recorded the ambient vertical velocity time histories as various aircraft repeatedly traversed normal to the grid. These digitized velocity traces produced an aircraft wake signature that could be used to infer the strength and lateral and vertical motion of the aircraft vortex pairs generating the traces.

In the Phase I tests the tower grid included anemometers for both horizontal and vertical velocities, with a total of 32 anemometers available for the analog-to-digital system employed to record the data. This study determined that the horizontal velocity signals would be easily polluted by any crosswind velocity component, giving a decidedly incorrect impression of the vortex position and strength. Also, the closeness of the tower grid (the towers were spaced 2.7 to 6.1 meters apart with seven towers) meant that no more than 20 to 40 seconds of data could be taken before the vortices would drift off the grid. Thus, in the Phase III tests the towers contained only vertical velocity anemometers, and were spaced uniformly apart at 6.1 meters (with ten towers). A longer sampling time was used to track the vortices across this wider tower grid.

The Phase I results suffer somewhat from not having long enough time histories to track the vortex pairs adequately (a crosswind velocity always blew the vortices off the tower grid). The Phase III results corrected the shorter experimental data times but contain decidedly noiser anemometer signals because of ambient downslope/upslope conditions. The local winds at Red Bluff resulted in stronger crosswind velocities, moving the vortices off the grid prematurely, and in some cases, negating the effect of the more widely spaced towers.

3. ANEMOMETER DATA COLLECTION

Table 1 summarizes the digitized tower data collected at Foresthill, Chico and Red Bluff. The corresponding tower grids are illustrated in scale in Figure 1, along with the aircraft flying over these grids. The size of the wakes and the positions of their vortex pairs (near the wing tips or the rotor edges) may then be qualitatively inferred.

All towers were instrumented as shown with propeller anemometers. The towers themselves were telescoping masts extended to several heights depending on the location and/or canopy cover. The anemometers were four-bladed propellers mounted vertically to measure the vertical velocity of the wake left by the traversing aircraft. The anemometers were connected to a data acquisition system consisting of an IBM portable PC with two Data Translation DT2801 auxiliary boards to sample and digitize 32 channels of analog voltage signals. Sampling was carried out at a rate of 100 samples/sec (each anemometer was sampled every 0.34 sec). The signals from all available anemometers were then used to infer the passage of the vortex pair generated as the wake of the traversing aircraft.

4. GENERALIZED ALGORITHM FOR DETERMINING VORTEX TRAJECTORIES

An aircraft wake may be represented by a simple vortex pair (with its image pair below the surface, Figure 2), each vortex of which may be characterized by a velocity field of the form

$$v = \frac{\Gamma}{2\pi} \frac{R}{\left(R_c^2 + R^2\right)} \qquad (1)$$

where

v = velocity magnitude

This report was orginally presented at the 19th National Conference on Agricultural and Forest Meteorology, March 7-10, 1989, at Charleston, South Carolina.

Γ = vortex circulation strength
R = radius from vortex center
R_c = vortex core radius, a constant

The resultant velocity at any point in the flow field (in particular, at an anemometer location) is then the algebraic sum of the velocity contributions from the four vortices acting on the flow. The aircraft vortex pair is located in a coordinate system relative to the tower grid (Figure 3). The wake model introduces four unknowns that must be deduced from the data in any run at any time at which data are collected. These unknowns are the vortex circulation strength Γ and the three spatial dimensions

h = height of the vortex pair

s = semispan of the vortex pair
d = offset from the leftmost tower

Aircraft wake physics are only approximated by the simple velocity law given in Eq. (1). Thus, the intent of the generalized analysis is to seek a solution for these four parameters so as to minimize the error in the velocity predictions at all of the anemometer locations. With four unknowns and many more anemometer locations, the problem may be cast into a least squares analysis by defining an error E as

$$E = \sum_{n=1}^{N} \left(w_n - \overline{w}_n\right)^2 \qquad (2)$$

Table 1

Tower Anemometer Conditions for Project WIND

Location	Foresthill	Chico	Red Bluff
Aircraft	AgHusky Bell Ranger 206	AgCat Hiller 12E	C-130 Bell Ranger 206
Runs	58 71	109	49
Tower Grids	A-E	F-H	I
Condition	Open Field Forested	Almond Orchard	Open Drainage

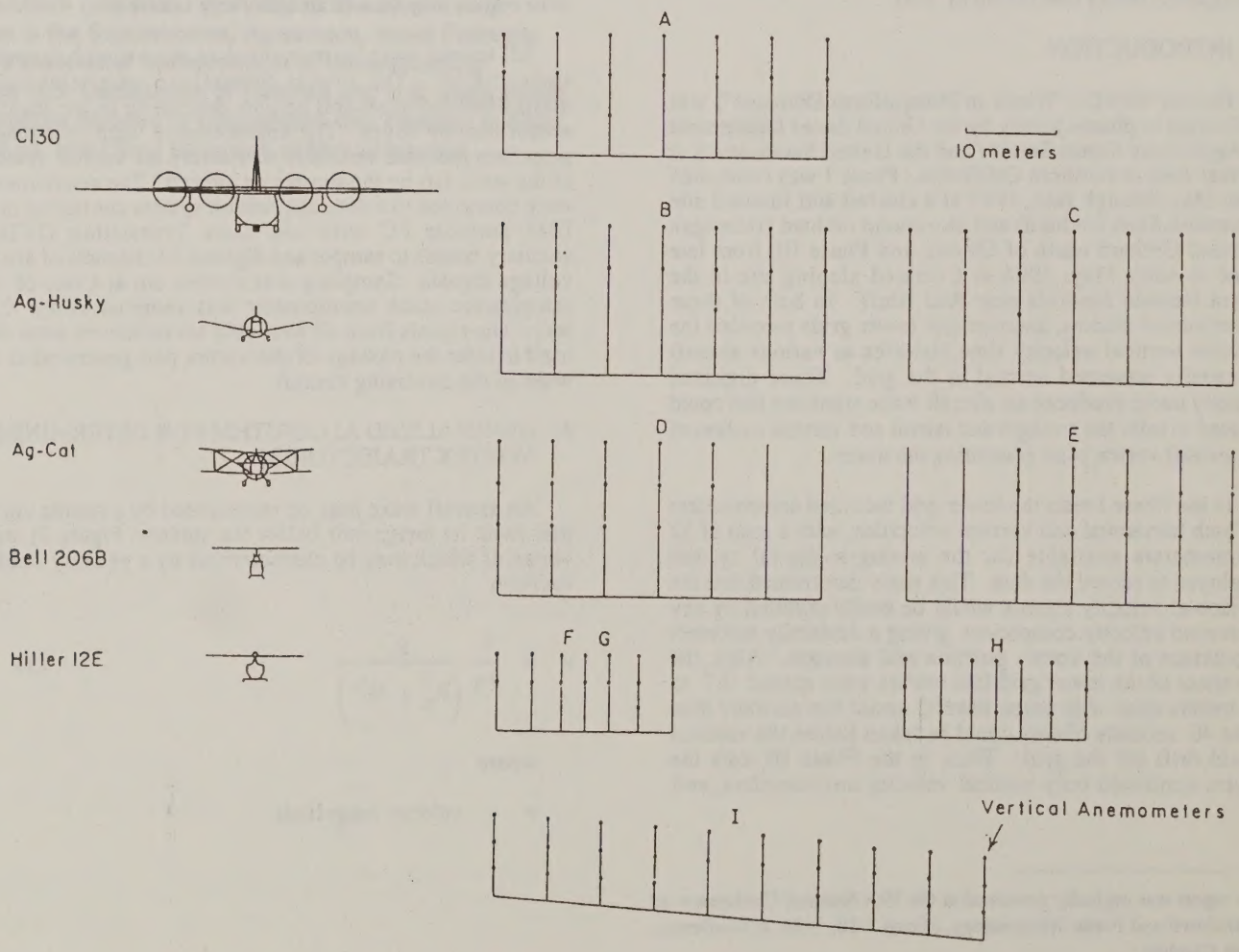

Figure 1: Scaled anemometer tower grids for Foresthill (A-E), Chico (F-H) and Red Bluff (I), right, and scaled cross-sections of the aircraft, left.

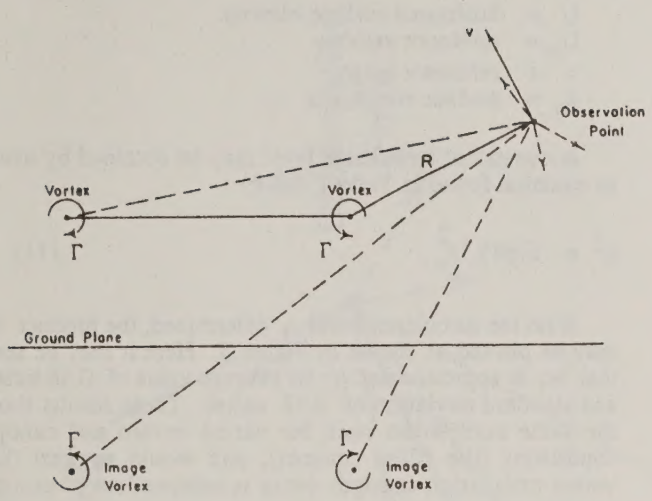

Figure 2: The composite velocity vector at an observation point found by summing the contributions of the aircraft vortex pair and its image system below the surface.

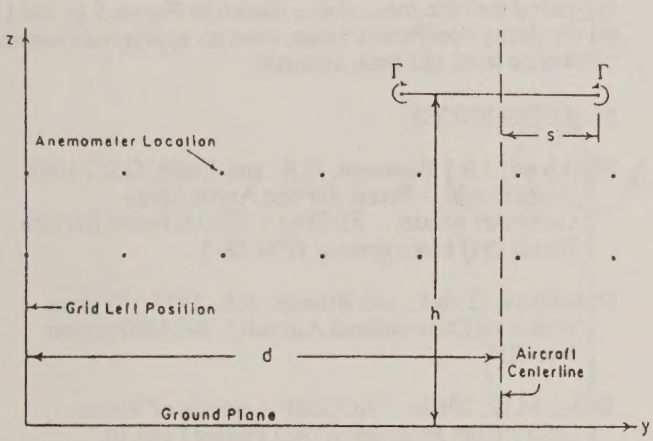

Figure 3: The aircraft vortex pair located relative to the anemometer tower grid.

where the overbar denotes the data, and N is the total number of anemometers. The error E is a positive definite quantity. The vertical velocities w are determined by summing the contributions of the four vortices in the model, calculated for specific values of the parameters Γ , h , s and d . The data $\overline{w}$ are found directly from the test results.

A crucial physical observation is made at this point: if the experimental data were normalized by any positive value, the resulting velocity vectors could still be used to infer the spatial position of the vortex pair in the anemometer field irrespective of the actual vortex circulation strength. This observation implies that locating the vortex pair involves the solution for h , s and d without regard to the value of Γ .

The approach used here normalizes the vertical velocities in the error equation by their respective root mean square velocities to give

$$E^* = \sum \left[\left(\frac{w_n}{w_{rms}} \right) - \left(\frac{\overline{w}_n}{\overline{w}_{rms}} \right) \right]^2 \qquad (3)$$

where

$$w_{rms} = \sqrt{\frac{1}{N} \sum w_n^2} \quad ; \quad \overline{w}_{rms} = \sqrt{\frac{1}{N} \sum \overline{w}_n^2}$$

Because the predicted vertical velocities are all linear in vortex circulation strength Γ , this modification to the error removes Γ from the equation for E^* and recasts the problem into one involving the parameters h , s and d .

Equation (3) for E^* is strongly nonlinear in h , s and d , but may be analytically differentiated with respect to these unknowns to give

$$F_h = \partial E^* / \partial h \; ; \; F_s = \partial E^* / \partial s \; ; \; F_d = \partial E^* / \partial d \qquad (4)$$

Clearly, when all three derivatives in Eq. (4) tend to zero, the slope of E^* also tends to zero and E^* reaches a local minimum. At any value set (h,s,d) , the local values of the F's in Eq. (4) may be determined analytically to generate partial derivatives of the form $\partial F/\partial h$, $\partial F/\partial s$, $\partial F/\partial d$ to construct the model equation for F of the form

$$\Delta F = \frac{\partial F}{\partial h} \Delta h + \frac{\partial F}{\partial s} \Delta s + \frac{\partial F}{\partial d} \Delta d \qquad (5)$$

The partial derivatives in this equation are known as influence coefficients. For any value set (h,s,d) , the values of the three partial derivatives and F may be generated. Since the solution requires F to tend to zero, the left-hand side of Eq. (5) may be specified by

$$\Delta F = - F \qquad (6)$$

The complete system may be seen to be a three-equation system for the incremental value set $(\Delta h, \Delta s, \Delta d)$ from Eq. (5), to add to the present value set (h,s,d) to drive F to zero and E^* to a minimum.

Once the value set (h,s,d) has been determined, the original error E may be differentiated to give

$$F_\Gamma = \partial E / \partial \Gamma = 0 \qquad (7)$$

to find the minimum of E and determine Γ . With the solution in hand for (Γ,h,s,d) , these values are used as initial guesses for the next time in the run being analyzed. All results presented here have been computed with a core size of $R_c = 0.15$ meters.

Figure 4 illustrates a typical result of the above procedure when applied to run 68 at Foresthill. All applicable runs (132 in number) are detailed in Teske (1988a).

5. DETERMINATION OF DECAY COEFFICIENT

The vortex strength decay model proposed is of the form

$$\Gamma(t) = \Gamma_o \exp\left(- \frac{bqt}{s} \right) \qquad (8)$$

where

Γ_o = initial vortex circulation strength at $t = 0$
b = decay coefficient
q = turbulence level

This expression was suggested as a possible model for vortex decay in the atmosphere in Donaldson and Bilanin (1975), with a decay coefficient value estimated to be 0.41 .

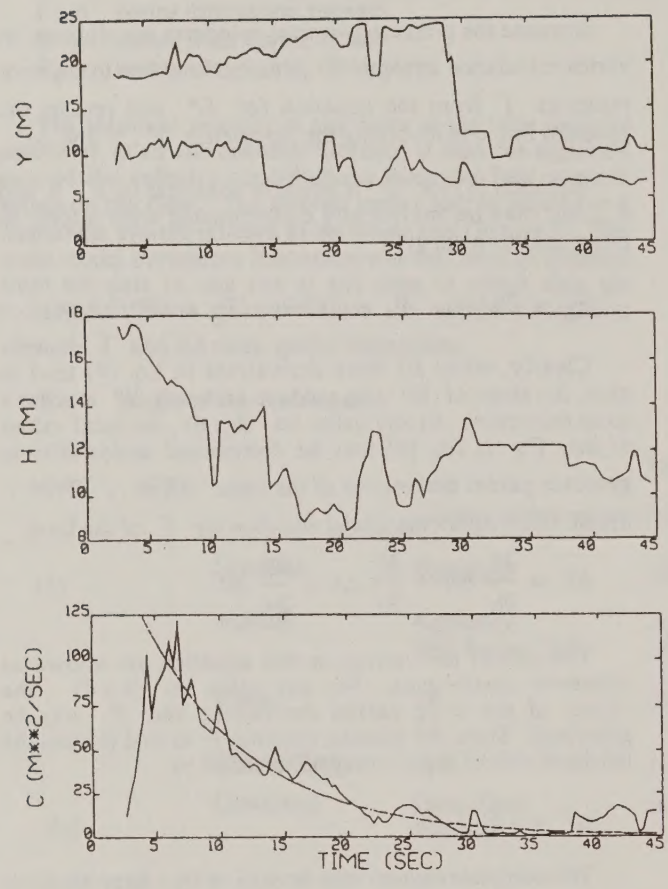

Figure 4: Foresthill run 68 generalized algorithm results for horizontal location of the vortices, top, vertical location of the vortices, middle, and circulation strength, bottom. The experimental curve fit is shown as the dashed curve.

A least squares approach was used to curve fit the vortex circulation strength data developed by the generalized algorithm. The vortex circulation strength profiles were fit to Eq. (8) by minimizing the logarithmic error

$$E = \sum [\, G - (A - Bt) \,]^2 \qquad (9)$$

over all applicable time increments in each run examined, where

G = logarithm of Γ
A = logarithm of Γ_o
B = bq/s

Equation (9) returns the best fit values for Γ_o and B for each run examined. A typical result is given by the dashed curve in Figure 4. Since the semispan s is known as a function of time from the generalized algorithm curve fit, the value of B could be used to infer the product bq .

In Phase I and Phase III, local horizontal winds were measured at several tower heights and used to estimate the turbulence level q for each run by a least squares curve fit to a neutral logarithmic profile of the form

$$U = U_o \ln (z/z_o) \qquad (10)$$

where

U = horizontal surface velocity
U_o = reference velocity
z = reference height
z_o = surface roughness

A consistent turbulence level may be obtained by using an equation found in Teske (1988b)

$$q^2 = 0.845\, U_o^2 \qquad (11)$$

With the turbulence level q determined, the product bq may be plotted as shown in Figure 5. Here it may be seen that bq is approximated by its average value of 0.56 m/sec and standard deviation of 0.32 m/sec. These results show the same correlation even for varied terrain and canopy conditions (the filled squares), and would suggest that vortex circulation strength decay is independent of canopy vegetation.

The present results suggest that a decay coefficient of near-zero to 2.0 may be used as input into AGDISP (Teske, 1988b) or FSCBG (Bjorklund, et.al., 1988). It is suggested that the mean curve shown in Figure 5 be used to set the decay coefficient value, once an appropriate ambient turbulence level has been assumed.

6. REFERENCES

Bjorklund, J.R., Bowman, C.R. and Dodd, G.C., 1988: "User Guide -- Forest Service Aerial Spray Computer Model -- FSCBG," USDA Forest Service Forest Pest Management FPM 88-5.

Donaldson, C. duP. and Bilanin, A.J., 1975: "Vortex Wakes of Conventional Aircraft," AGARDograph No. 204.

Teske, M.E., 1988a: "AGDISP Analysis of Vortex Decay from Program WIND Phases I and III," Continuum Dynamics, Inc. Technical Note 88-06.

Teske, M.E., 1988b: "AGDISP Mod 5 User Manual," Continuum Dynamics, Inc. Technical Note 88-09.

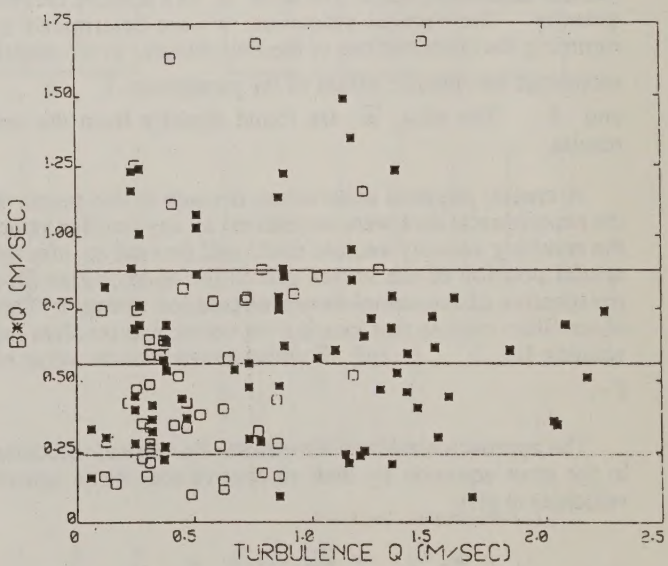

Figure 5: The behavior of the product bq with turbulence level q . Each square represents one of the 132 applicable test runs. The solid curve is the mean of the data; the dashed curves represent the standard deviation. The filled squares are data from canopy conditions.

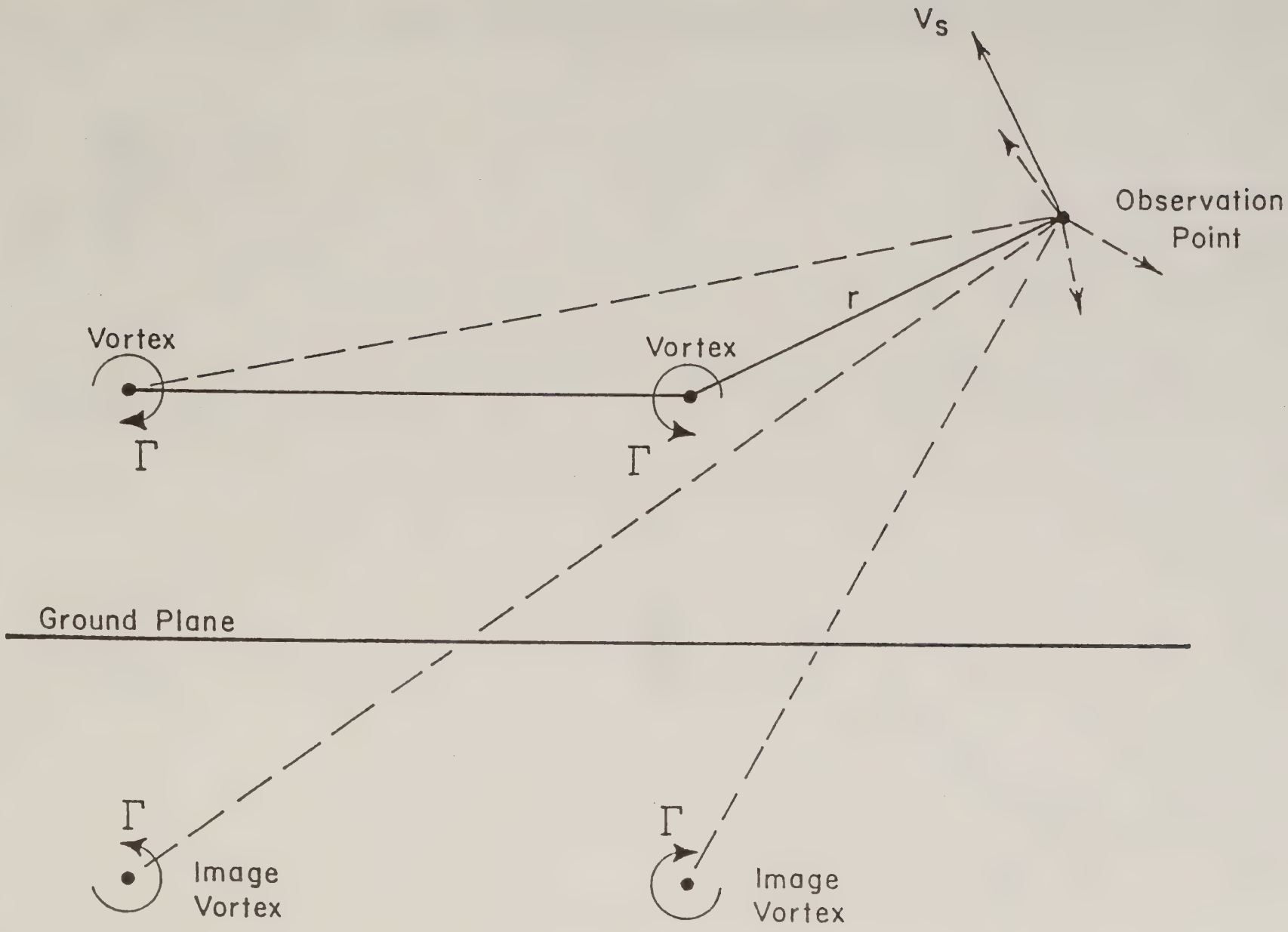

Figure 2-4. The composite velocity vector at an observation point found by summing the contributions of the aircraft vortex pair and its image system below the ground plane.

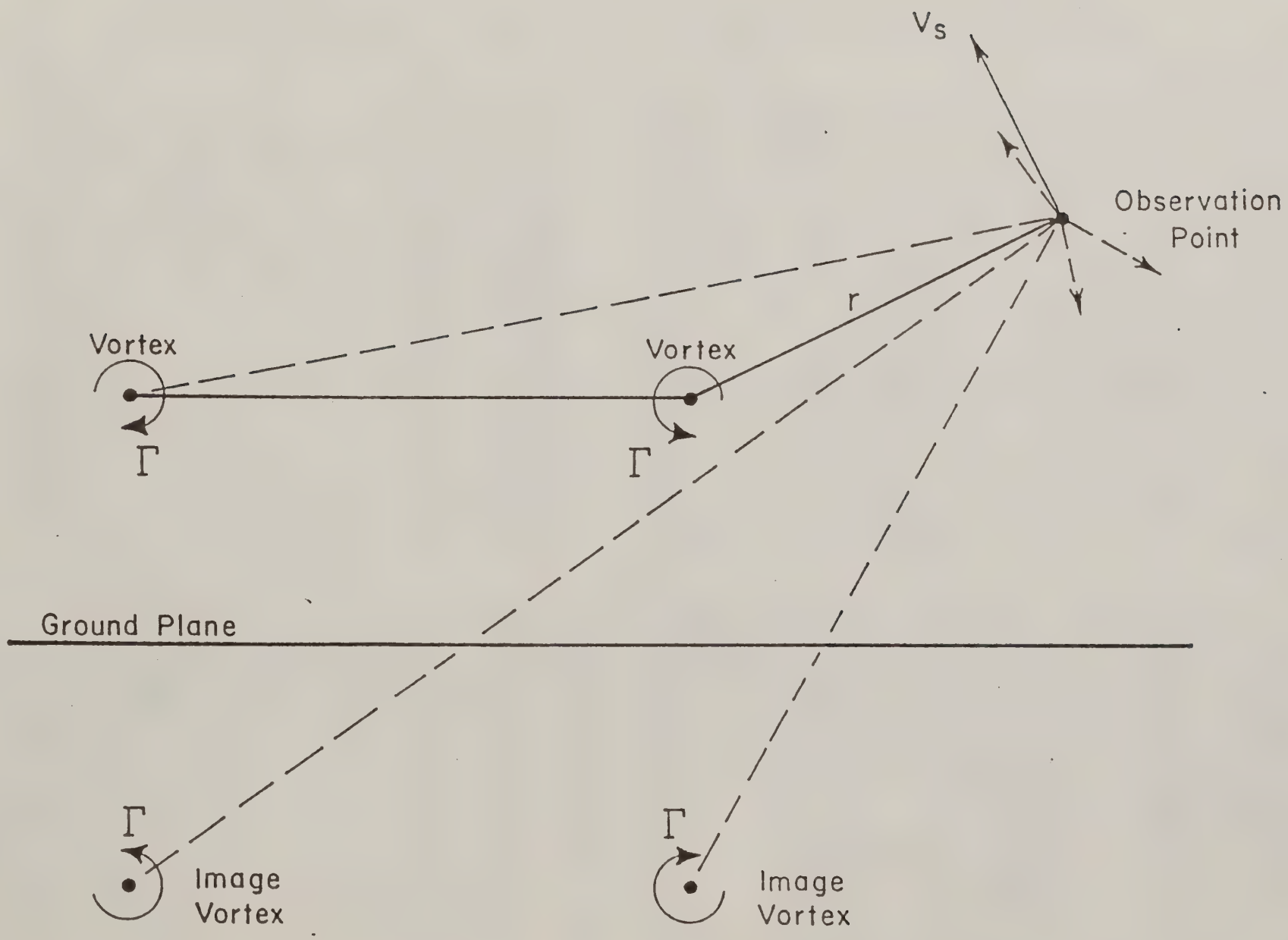

Figure 2-4. The composite velocity vector at an observation point found by summing the contributions of the aircraft vortex pair and its image system below the ground plane.

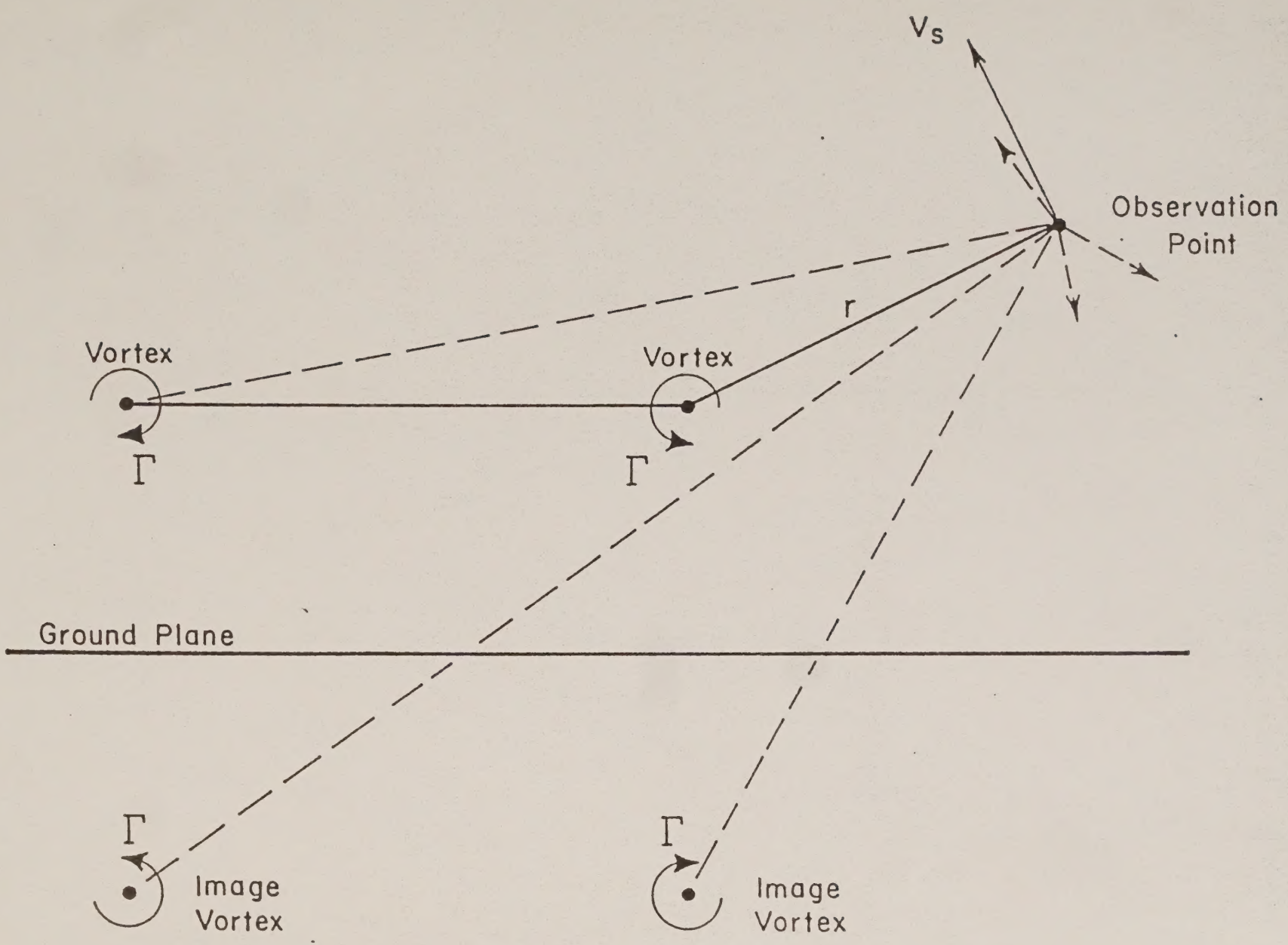

Figure 2-4. The composite velocity vector at an observation point found by summing the contributions of the aircraft vortex pair and its image system below the ground plane.